JCTC Journal of Chemical Theory and Computation

ARTICLE

pubs.acs.org/JCTC

Eigensystem Representation of the Electronic Susceptibility Tensor for Intermolecular Interactions within Density Functional Theory

A. Scherrer, V. Verschinin, and D. Sebastiani*

Dahlem Center for Complex Quantum Systems, Physics Department, Free University Berlin, Arnimallee 14, 14195 Berlin, Germany

ABSTRACT: We present an efficient implementation of the electronic susceptibility tensor within density functional theory. The susceptibility is represented by means of its eigensystem, which is computed using an iterative Lanczos diagonalization technique for the susceptibility tensor within density functional perturbation theory. We show that a representation in a finite basis of eigenstates is sufficiently accurate to compute the linear response of the electronic density to external potentials. Once the eigensystem representation is computed, the actual response computation can be done at very low computational cost. The method is applied to the water molecule in a dipole field as a benchmark system. The results illustrate the potential of the approach for the first-principles calculation of supramolecular interactions in complex disordered systems in the condensed phase.

1. INTRODUCTION

Most spectroscopic techniques in physics and chemistry measure the response of the investigated system to an external field, that is, an external modification of the environmental situation. More specifically, optical spectroscopies use an electric field, while magnetic resonance spectroscopies work on the basis of a magnetic field. In many cases, the response of the system is primarily of electronic nature, meaning that the electrons in the system change their quantum state. This change in state then emits or absorbs, for example, radiation, which in turn is measured by the experiment.

In many cases, the external field is small as compared to the typical electronic energy spectrum, in particular excitation energies. In such cases, it is possible to consider the external field as a small perturbation, and within the context of quantum mechanics, perturbation theory can be applied to determine the linear response of the electronic subsystem to the perturbation. In this framework, the induced change in the electronic orbitals is assumed to be proportional to the strength of the external field. Within the framework of first-principles electronic structure theories, in particular density functional theory (DFT[1−3]), this linearity also applies to the electronic density, giving rise to density functional perturbation theory.[4−7]

It is straightforward to show (see section 3) that the linear response of the electron density to a (nonimaginary) local perturbation $\hat{H}^{(1)}$ can be written as

$$n^{(1)}(\mathbf{r}) = \int \mathrm{d}\mathbf{r}'\, \chi(\mathbf{r},\mathbf{r}')H^{(1)}(\mathbf{r}') \qquad (1)$$

with a universal linear response function $\chi(\mathbf{r},\mathbf{r}')$ (independent of $\hat{H}^{(1)}$). $\hat{\chi}$ is formally a tensor in a continuous basis and therefore difficult to handle in practice. In this work, we have developed an implementation similar to a very recently published approach for the related problem of the static dielectric matrix[8−10] to approximate the susceptibility tensor by expansion in its eigensystem representation. The method uses repeated calculation of the response in eq 1 via density functional perturbation theory (DFPT).[11,12]

It turns out that the spectrum of $\chi(\mathbf{r},\mathbf{r}')$ converges sufficiently quickly to allow for an efficient representation of the tensor in its finite eigensystem representation. This assumption has already been validated by several recent studies,[13−18] in which a similar scheme was used to compute the dielectric response matrix, the RPA correlation and self-energies, as well as optical spectra of condensed-phase systems.

It is known that, in addition to dielectric response properties, a perturbation theory-based Ansatz is in principle also capable of representing supramolecular interaction energies to a very high accuracy.[19,20] In this Article, we develop the electronic linear response approach within density functional perturbation theory for subsequent application to a perturbative calculation of such intermolecular interactions.

Complementary to the existing implementation by Galli et al.,[9,10,13] we specifically aim at computing interaction energies and atomic forces between the components of supramolecular systems, for example, complex liquids (water, ionic liquids) or molecular crystals. Our present implementation has not yet been optimized to tackle such systems in a black-box manner, but our results show that the approach yields highly accurate results. We believe that the method can be used to calculate ab initio level interaction energies at a very low computational cost.

2. THEORY

2.1. Susceptibility Tensor with DFPT. Within DFPT,[6,11,12] all relevant quantum quantities (Hamiltonian, orbitals, density) are expanded expressed by their unperturbed and perturbed components, for example, $\hat{H} = \hat{H}^{(0)} + \lambda\hat{H}^{(1)}$. The first-order response of the orbitals can formally be calculated by

$$|\psi_i^{(1)}\rangle = -(\hat{H}^{(0)} - E_i^{(0)})^{-1}P_e\hat{H}^{(1)}|\psi_i^{(0)}\rangle \qquad (2)$$

with $P_e = 1 - \Sigma_{j,\mathrm{occ}}|\psi_j^{(0)}\rangle < \psi_j^{(0)}|$. Assuming that the perturbation

Received: September 30, 2011
Published: November 23, 2011

Hamiltonian $\hat{H}^{(1)}$ is local, the resulting density response is given by eq 1 with

$$\chi(\mathbf{r},\mathbf{r}') = -\sum_{i=1}^{N} [\psi_i^{*(0)}(\mathbf{r})\langle\mathbf{r}|(\hat{H}^{(0)} - E_i^{(0)})^{-1}P_c|\mathbf{r}'\rangle\psi_i^{(0)}(\mathbf{r}') + \text{cc}] \tag{3}$$

This expression of $\chi(\mathbf{r},\mathbf{r}')$ does not provide a feasible way for its calculation because the dimensions of $\chi(\mathbf{r},\mathbf{r}')$ are continuous and any suitable real-space discretization would yield matrices with dimensions too large for explicit matrix inversions. However, from eq 3 it is apparent that $\chi(\mathbf{r},\mathbf{r}')$ is real and symmetric. Hence, $\hat{\chi}$ can be expressed on the basis of its eigenstates $|\chi_\xi\rangle$, defined via $\hat{\chi}|\chi_\xi\rangle = \chi_\xi|\chi_\xi\rangle$, as

$$\hat{\chi} = \sum_\xi |\chi_\xi\rangle\chi_\xi\langle\chi_\xi| \tag{4}$$

It is important to note that in this decomposition the contribution of the eigenstates is weighted by their eigenvalues χ_ξ. Eigenstates with zero eigenvalue do not contribute to the summation and can thus be omitted. For nonmetallic systems, the spectrum $\{\chi_\xi\}$ is bound from above, because the expression $(\hat{H}^{(0)} - E_i^{(0)})^{-1}$ in eq 2 is limited by the inverse of the HOMO−LUMO energy gap. Hence, if the spectrum decays sufficiently fast, most of the eigenvalues may be omitted to a good approximation; it is a valid approximation to omit most of the eigenstates.

$$\hat{\chi} \approx \sum_\xi^{N_{\max}} |\chi_\xi\rangle\chi_\xi\langle\chi_\xi| \tag{5}$$

With this at hand, the approximate determination of $\hat{\chi}$ turns into the problem of finding the eigenvectors with the corresponding largest eigenvalues.

2.2. Lanczos Diagonalization. For the calculation of the eigenvectors $|\chi_\xi\rangle$ corresponding to the largest eigenvalues χ_ξ, we resort to an iterative diagonalization scheme (Lanczos, see section 3). The Lanczos method is a Krylov-space approach, which requires the repeated application of the operator that shall be diagonalized to a given vector $|\mu\rangle$. For our electronic susceptibility tensor, one such application $|\nu\rangle = \hat{\chi}|\mu\rangle$ corresponds to solving the DFPT eq 2 once with $\mu = \hat{H}^{(1)}$ for $\nu = n^{(1)}$. This operation is hence straightforward and requires a computational effort similar to a ground-state total energy calculation.

2.3. Polarizability. One of the physical observables closely related to the electronic susceptibility tensor $\hat{\chi}$ is the electric polarizability tensor $\alpha = \mathrm{d}\mathbf{p}/\mathrm{d}\mathbf{E}$, where $\mathbf{E}$ is a homogeneous electric field acting as a perturbation. The induced polarization $\delta\mathbf{p}$ is given by

$$\delta\mathbf{p} = \int \mathrm{d}\mathbf{r}\, \mathbf{r} n^{(1)}(\mathbf{r}) \tag{6}$$

$$= \int \mathrm{d}\mathbf{r}\, \mathbf{r} \int \mathrm{d}\mathbf{r}'\, \chi(\mathbf{r},\mathbf{r}') e\mathbf{E}_0 \cdot \mathbf{r}' \tag{7}$$

Using the eigenstate representation of $\hat{\chi}$ and the first moments of its eigenstates $\beta_{\mu,\xi} = \int \mathrm{d}\mathbf{r}\, \chi_\xi(\mathbf{r}) r_\mu$ gives

$$\alpha_{\mu\nu} = \sum_\xi \chi_\xi e \int \mathrm{d}\mathbf{r}\, \chi_\xi(\mathbf{r}) r_\mu \int \mathrm{d}\mathbf{r}'\, \chi_\xi(\mathbf{r}') r_\nu' \tag{8}$$

$$= \sum_\xi \chi_\xi e \beta_{\mu,\xi}\beta_{\nu,\xi} \tag{9}$$

Thus, the electric polarizability α can be computed directly from the susceptibility eigenfunctions and can therefore serve as a perfect tool measure for the convergence analysis for the finite expansion eq 5.

3. IMPLEMENTATION

3.1. Lanczos Algorithm. Formally, the numerical problem to solve is the determination of the eigenvectors with the largest eigenvalues of an unknown Hermitian matrix A with only its action on a vector available. This matrix A is not known explicitly, but only by its action on a given vector. In this work, this diagonalization task is done using the Hermitian Lanczos algorithm. It is an iterative method to obtain approximate eigenvectors, and the corresponding orthogonal projection $B_m \in \mathbb{C}^{m\times m}$ of a Hermitian matrix $A \in \mathbb{C}^{n\times n}$ with $m \ll n$ uses Krylov subspaces $\mathscr{K}_m$ to iteratively create the needed subspace needed for the orthogonal projection.[21,22]

The implemented version of the algorithm is

- Choose $\mathbf{v}_1$ with $|\mathbf{v}_1| = 1$. Set $\beta_1 = 0$, $\mathbf{v}_0 = 0$.
- Iterate for $j = 1, 2, \ldots, m$

$$\tilde{\mathbf{w}}_j = A\mathbf{v}_j \tag{10}$$

$$\alpha_j = \tilde{\mathbf{w}}_j \cdot \mathbf{v}_j \tag{11}$$

$$\mathbf{w}_j = \hat{P}\tilde{\mathbf{w}}_j \tag{12}$$

$$\beta_{j+1} = |\mathbf{w}_j| \tag{13}$$

$$\mathbf{v}_{j+1} = \mathbf{w}_j/\beta_{j+1} \tag{14}$$

The orthonormalization $\hat{P}$ in eq 12 is performed with respect to all vectors already found. With exact arithmetics, only the first two vectors would be sufficient.

The calculated vectors $\mathbf{v}_j$ form an orthonormal basis $V_m = [\mathbf{v}_1, \mathbf{v}_2, \ldots, \mathbf{v}_m]$, and the resulting orthogonal projection matrix $B_m = V_m^\dagger A V_m$ has the desirable properties of being real, tridiagonal, and symmetric. The calculated coefficients α_j and β_j are its diagonal and off-diagonal elements, respectively. Because $m \ll n$, the diagonalization of the Rayleigh−Ritz procedure is numerically feasible and can be done with, for example, a QR-decomposition with scaling that scales as $\mathscr{O}(m^2)$. The resulting eigenvectors $\mathbf{u}_j$ of B_m are called Ritz vectors and contain the coefficients for the approximate expansion of the original eigenvectors of the matrix A in the basis V_m. The approximate eigenvectors are calculated ordered by the absolute value of their corresponding eigenvalues as desired for their application in this context. The Lanczos algorithm yields the approximate eigenvectors in the order of decreasing eigenvalues. This means that the extremal part of the spectrum is obtained first, which fits the idea of the representation according to eq 5.

3.2. Underlying Electronic Hamiltonian. The concepts presented so far are general and independent of the electronic structure method chosen. In this work, we use DFT and obtain the response in eq 1 via density functional perturbation theory[12] in the implementation framework of the CPMD software.[23] We use separable norm-conserving pseudopotentials,[24] the BLYP

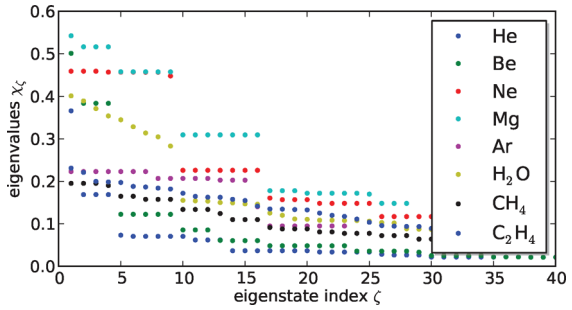

Figure 1. First eigenvalues of the lightest closed-shell atoms and the molecules H_2O, CH_4, and C_2H_4.

gradient corrections functionals, and a PW cutoff of 70 Ry with simple cubic system symmetry. The cell sizes are 7 Å for isolated atoms and 10 Å for molecular systems.

3.3. Convergence. Mathematically speaking, the choice of the initial vector determines the shape and the maximum dimension of the calculated Krylov subspaces, that is, also the number of possible iterations m. Ideally, the start vector should be a linear combination of all relevant eigenvectors, that is, all eigenvectors with significantly nonzero eigenvalue. In our particular case of the electronic susceptibility tensor, we have found that the electronic ground-state density shifted by q/Ω (with $q = \int_\Omega d\mathbf{r}\ \rho(\mathbf{r})$) is sufficient as an initial vector a good choice. However, the impact of nonexact arithmetics effectively increases the maximum dimension and reduces the sensitivity of the method to the initial conditions.

At any iteration of the Lanczos cycle in an actual calculation, only a part of the Ritz vectors u_j are numerically accurate eigenvectors of A. A suitable measure for the quality of a given u_j is the absolute value of its last element u_{jm}. This element represents the overlap of the true eigenvector with the latest calculated vector $\mathbf{v}_m$. We have verified empirically that this convergence criterion is an excellent and reliable choice for our purposes.

We have set the convergence criterion for the eigenvectors to $u_{jm} \leq 10^{-5}$. After about 5000 Lanczos iterations, we find that typically one-half of the resulting Ritz vectors u_j can be considered as converged. This ratio remains approximately constant also for subsequent iterations.

4. RESULTS

To illustrate the validity and the versatility of the approach, we have applied our finite basis representation of the electric susceptibility tensor to several complementary molecular systems. Specifically, we have computed the following:

- the three-dimensional shape of the eigenstates and decay of the eigenvalues for isolated atoms of different elements (He, Ne, Ar, Be, Mg) and small molecules (H_2O, CH_4, C_2H_4);
- the polarizability of H_2O, CH_4, C_2H_4, and C_2H_6; and
- the induced polarization of Be, H_2O, CH_4, and C_2H_4 due to the inhomogeneous electric field of a salt ion pair Na^+Cl^-.

4.1. Eigenstates and Eigenvalues. To obtain an idea of the numerical shape of the spectrum of $\hat{\chi}$, we have plotted the initial eigenvalues for a set of isolated atoms and molecules in Figure 1.

For the single atoms, the convergence is stepwise with several eigenvalues of equal or similar size. The decay of the eigenvalue spectrum resembles that of the energy spectrum of Z/r-type Coulomb potentials. Such Z/r potentials yield degenerate states

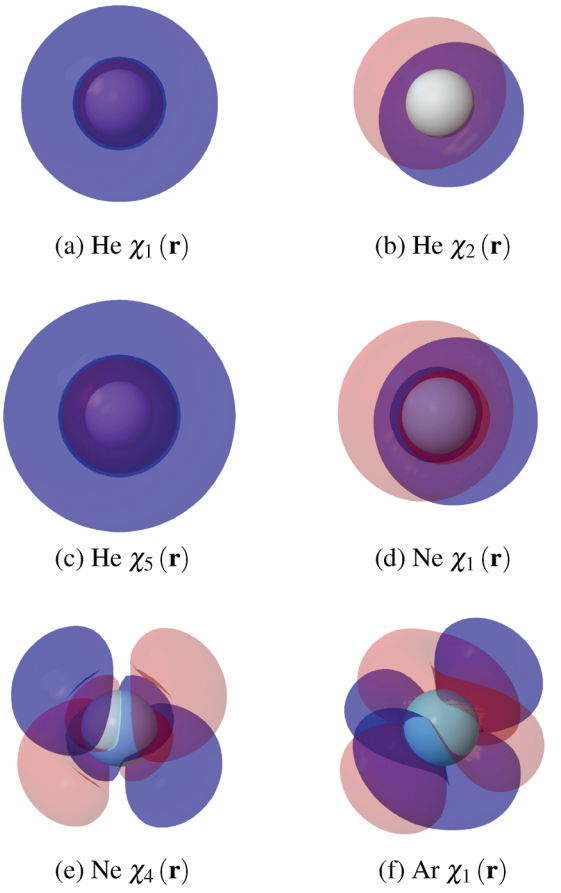

Figure 2. First eigenstates of He, Ne, and Ar. The isosurface plot is done with Jmol using cutoffs of +0.01 (red) and −0.01 (blue).

with characteristic symmetry properties. The eigenstates of the susceptibility tensor turn out to exhibit very similar symmetries, as depicted in Figure 2 for He, Ne, and Ar. The analogy to the more familiar orbital model is obvious.

The first eigenstate of helium is spherically symmetric and nondegenerate, whereas the 3-fold degeneracy of the second to forth eigenstate of helium and the first three eigenstates of neon come along with a symmetry similar to p-orbitals of the hydrogen atom. The analogy may not be applied strictly as shows the example of argon, where the first eigenvalue is 7-fold degenerate, which has no trivial counterpart in the hydrogen case.

Naturally, the degeneracies observed for spherically symmetric atoms are lifted for less symmetric molecules such as H_2O or C_xH_y. The eigenvalues of the latter do not show exact degeneracies. A selection of the first eigenstates is plotted in Figure 3. The symmetries of the eigenstates are related to the symmetries of the molecule. Furthermore, the parity changes with respect to the different symmetry axes, which is relevant for the convergence properties in the following. Generally, the eigenstates exhibit different parity properties for the different molecular symmetry axes.

The eigenstates of higher order have more complex symmetries. As an example, the 30th eigenstates of Be and H_2O are shown in Figure 4. The overall tendency is an increase in the number of nodes, that is, more oscillations and steeper slopes. Again, this is analogous to the behavior of higher orbitals in the orbital model with higher quantum numbers.

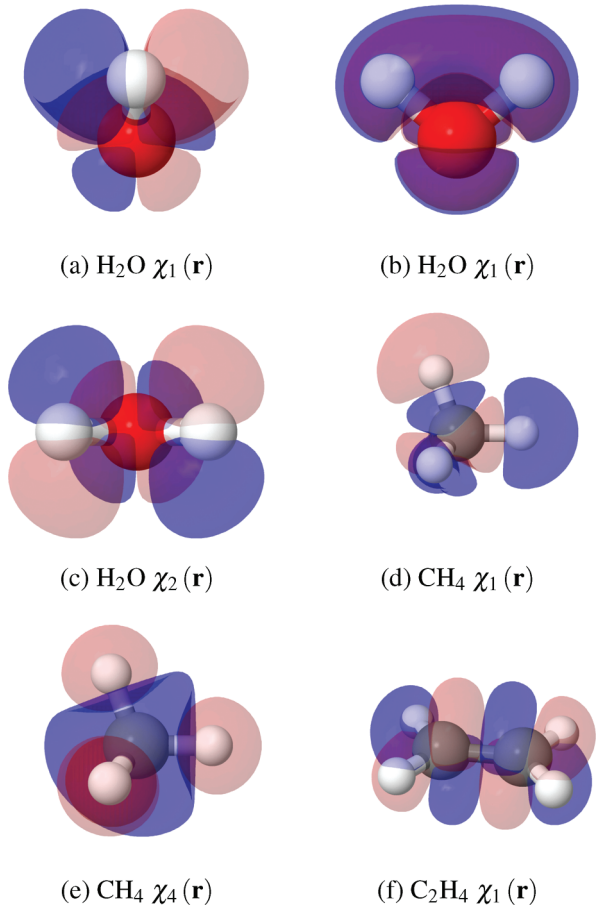

Figure 3. First eigenstates of H_2O, CH_4, and C_2H_4.

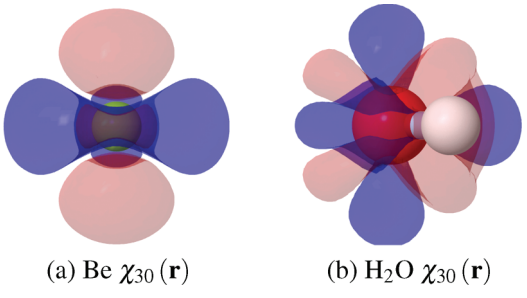

Figure 4. 30th eigenstate of Be and H_2O.

The quick decay of the spectrum of $\hat{\chi}$ is an important property that we observed in all considered systems. It allows the truncation of the summation according to eq 5 with a moderate value for N_{max}. The asymptotic behavior of the eigenvalues is depicted in Figure 5 and shows an algebraic decline. The difference between Be and the molecules indicates that more complex systems converge more slowly. To a certain extent, the decay characteristics are determined by the total number of occupied orbitals. This effect has already been discussed by Galli.[13]

Because the eigenstates have the character of a density response, they must obey charge conservation. This means that $\int d\mathbf{r}\, \chi_\nu(\mathbf{r}) \stackrel{!}{=} 0$ for all eigenstates. We have checked numerically that this charge conservation property is fulfilled up to machine precision of 10^{-14}.

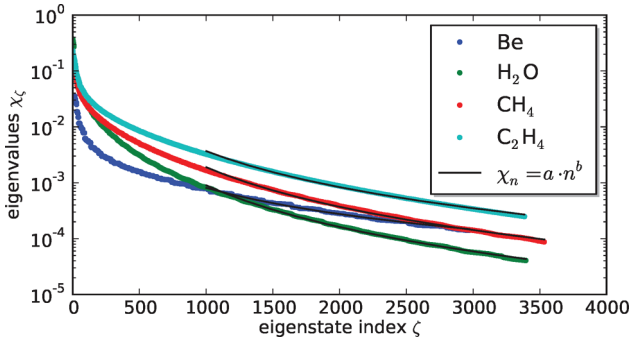

Figure 5. Asymptotic behavior of eigenvalues. The fitting parameters for the systems are a = (3.7, 10.1, 10.0, 9.2) and b = (−1.6, −2.5, −2.4, −2.1) for Be, H_2O, CH_4, and C_2H_4, respectively.

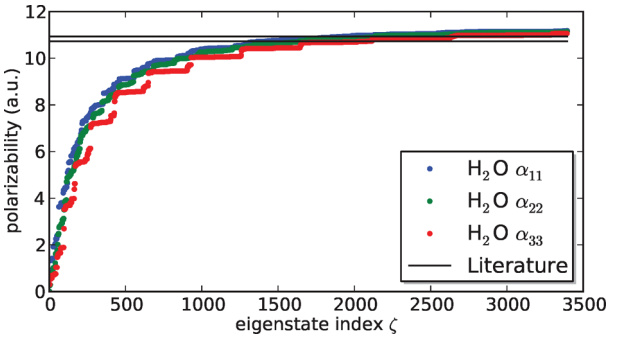

Figure 6. Main diagonal elements of the polarizability tensor of H_2O. The given literature values are for DFT calculations with GGA functional.[12,25]

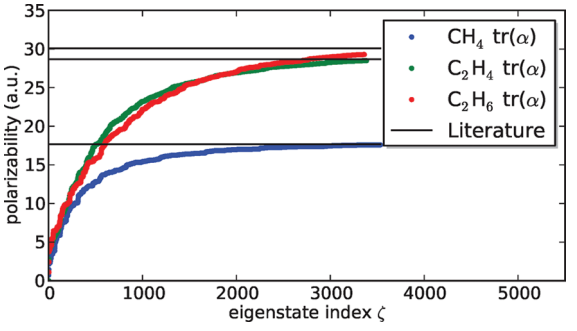

Figure 7. Polarizability of CH_4, C_2H_4, and C_2H_6. Literature values are as in Figure 6.

4.2. Polarizability. The polarizability in the presence of a homogeneous infinitesimal electric field can be computed with standard DFPT[12] and via eq 9. In Figure 6, we illustrate the numerical convergence of the susceptibility-based expression to the literature value from refs 12,25. The graph shows several plateaus, which indicates that many of the eigenstates have a vanishing contribution to the polarizability. This is due to the symmetry of the eigenstates with respect to the direction of the field. If the parity of χ_ν is even in a given direction, the corresponding β_ν vanishes.

As a further benchmark, we have computed the traces of the polarizability tensor $tr(\alpha)$ for the organic molecules CH_4, C_2H_4, and C_2H_6. The convergence as a function of the total number of

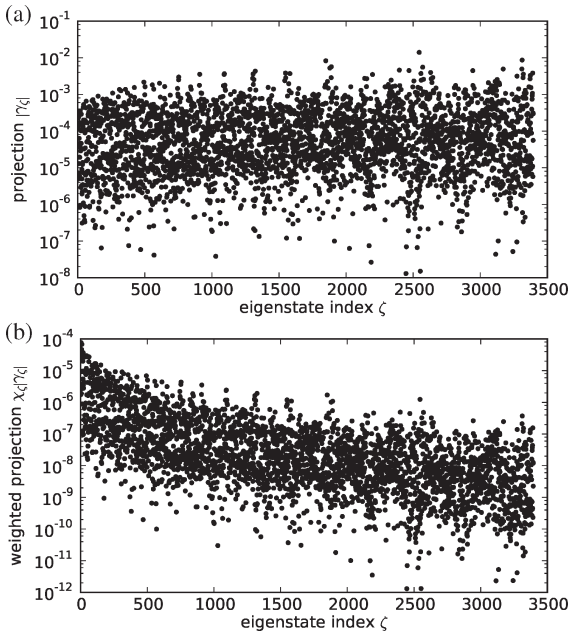

Figure 8. Projection coefficients and weighted projection coefficients of the perturbing potential on the eigenstates of H_2O.

eigenstates is depicted in Figure 7. Again, the convergence depends moderately on the number of electrons in the molecule.

Summarizing the results in this section, we conclude that the susceptibility in its low-rank approximation in eq 5 is able to represent the electronic polarizability tensor for our set of small molecules to a very good accuracy.

4.3. Polarization by Finite Charges. As a first step toward the description of intermolecular interaction, we have looked at the polarization of a water molecule in the inhomogeneous electrostatic field of a Na^+Cl^- ion pair. Denoting the potential of the two ions by $H^{(1)} := V_{[Na+Cl^-]}^{Coulomb}$, the response of a system X (e.g., H_2O) requires the calculation of the projections $\chi_{\zeta,[X]}$ of the perturbing potential on the eigenstates of the system X:

$$\gamma_{\zeta,[X,Na^+Cl^-]} := \langle \chi_{\zeta,[X]} | V_{[Na^+Cl^-]}^{Coulomb} \rangle \tag{15}$$

Combining eqs 4, 1, and 15, the density response is given as

$$n^{(1)}_{[X,Na^+Cl^-]}(\mathbf{r}) = \sum_\zeta \chi_{\zeta,[X]}(\mathbf{r}) \chi_{\zeta,[X]} \gamma_{\zeta,[X,Na^+Cl^-]} \tag{16}$$

For a water molecule, the resulting coefficients $\gamma_{\zeta,[H_2O,Na+Cl-]}$ are depicted in Figure 8a. Up to 3000 eigenstates, no particular trend is observed. In fact, the coefficients $\gamma_{\zeta,[H_2O,Na+Cl-]}$ show a broad scattered distribution between 10^{-3} and 10^{-6}.

The contribution of a particular eigenstate in eq 16 is proportional to the product of the projection coefficient and its corresponding eigenvalue; this product is depicted in Figure 8b. While the width of the distribution of the weighted coefficients remains constant for the whole spectrum, the center of the distribution decreases for large eigenstate indices ζ. However, the decay is relatively slow, even after several thousand eigenstates. Together with the large width of the weighted projection band, this indicates that at the present stage of the implementation, there is still a large part of the computational effort spent on insignificant eigenstates. This problem is related to the mutual symmetry properties of eigenstates and the perturbation as in the case of the polarizability tensor.

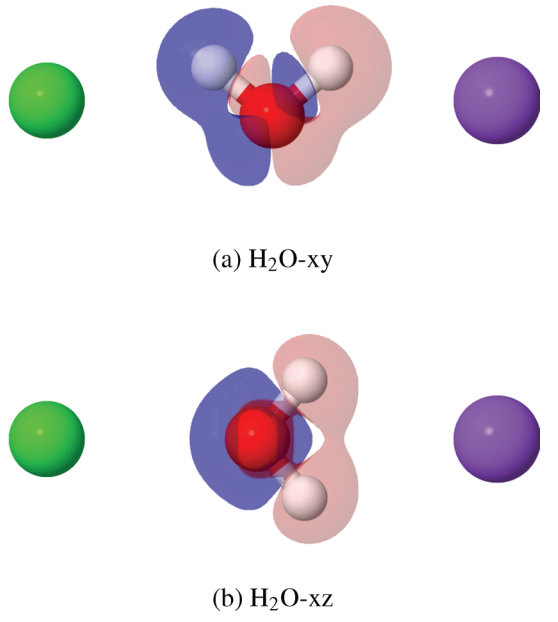

Figure 9. Linear response densities for H_2O for different orientations in the Na^+Cl^- potential, calculated via DFPT (left, Cl^-; right, Na^+).

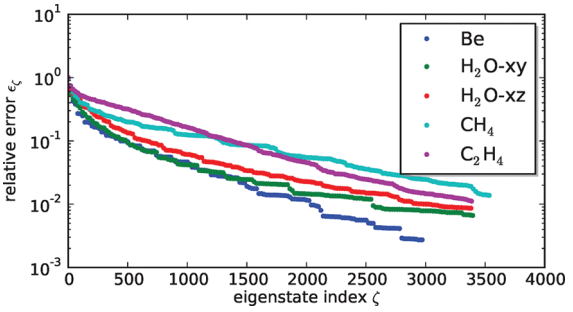

Figure 10. Relative error of the approximated $\hat{\chi}$-linear response to the directly calculated one for Be, H_2O, CH_4, and C_2H_4.

We now want to compute the actual linear response density of our water molecule, that is, the charge displacement due to the field of the Na^+Cl^- atoms. This quantity is obtained by summing all data points in Figure 8b. This response density is illustrated in Figure 9, showing the shift of the electric cloud away from the Cl^- side toward the Na^+ ion. Interestingly, the opposite polarization is observed locally around the oxygen atom (Figure 9a). This is a purely quantum effect, which cannot be reproduced by a simple "polarizable charge distribution" model.

When using eq 16 to compute this charge displacement, the sum has to be truncated. To quantify the approximation error due to the truncation, we compare the result of eq 16 $n^{(1)}(\zeta)$ with the response calculated directly via DFPT n^{DFPT} in dependency of the truncation index ζ:

$$\varepsilon(\zeta) = \frac{|n^{DFPT} - n^{(1)}(\zeta)|_2}{|n^{DFPT}|_2} \tag{17}$$

The asymptotic behavior of this relative error is depicted in Figure 10. The convergence is mainly smooth rippled. The results for the different orientations of H_2O show a slight difference, which is due to the different symmetry properties of the eigenstates with respect to the symmetry of the perturbing

dx.doi.org/10.1021/ct200695y | J. Chem. Theory Comput. 2012, 8, 106–111

potential. The convergence is similar for all molecules considered here. Only a slight dependence on the complexity of the system is observed. Depending on this complexity, a relative error of ∼1% may be achieved from about 3000−4000 converged eigenstates.

5. CONCLUSION

We have used a finite representation of the electronic linear susceptibility tensor for the computationally efficient calculation of molecular interactions, in particular electrostatic polarization, within density functional theory. Our results show that it is possible to compute such polarization effects with arbitrary accuracy for the response density $\delta\rho(\mathbf{r})$, typically 1% when considering about 3000 eigenstates.

The calculation of the response due to an arbitrary perturbation requires only few vector multiplications and no actual wave function optimizations. This means that the approach may be able to achieve virtually exact DFT interaction energies at a fraction of the computational cost. The application of actual supramolecular systems still needs further implementation efforts, which are presently underway.

AUTHOR INFORMATION

Corresponding Author

*E-mail: daniel.sebastiani@fu-berlin.de.

Note

The authors declare no competing financial interest.

ACKNOWLEDGMENT

We are grateful to Michele Parrinello for valuable discussions, which initiated this project. This work was financially supported by the Deutsche Forschungsgemeinschaft under grants Se 1008/5 and Se 1008/6.

REFERENCES

(1) Hohenberg, P.; Kohn, W. *Phys. Rev.* **1964**, *136*, B864.
(2) Kohn, W.; Sham, L. J. *Phys. Rev.* **1965**, *140*, A1133.
(3) Jones, R. O.; Gunnarsson, O. *Rev. Mod. Phys.* **1989**, *61*, 689–746.
(4) Gonze, X. *Phys. Rev. A* **1995**, *52*, 1096.
(5) Gonze, X.; Allan, D. C.; Teter, M. P. *Phys. Rev. Lett.* **1992**, *68*, 3603.
(6) Gonze, X.; Vigneron, J. P. *Phys. Rev. B* **1989**, *39*, 13120.
(7) Giannozzi, P.; de Gironcoli, S.; Pavone, P.; Baroni, S. *Phys. Rev. B* **1991**, *43*, 7231.
(8) Hamel, S.; Williamson, A. J.; Wilson, H. F.; Gygi, F.; Galli, G.; Ratner, E.; Wack, D. *Appl. Phys. Lett.* **2008**, *92*, 043115.
(9) Lu, D.; Gygi, F.; Galli, G. *Phys. Rev. Lett.* **2008**, *100*, 147601.
(10) Wilson, H. F.; Gygi, F.; Galli, G. *Phys. Rev. B* **2008**, *78*, 113303.
(11) Baroni, S.; de Gironcoli, S.; del Corso, A.; Giannozzi, P. *Rev. Mod. Phys.* **2001**, *73*, 515.
(12) Putrino, A.; Sebastiani, D.; Parrinello, M. *J. Chem. Phys.* **2000**, *113*, 7102–7109.
(13) Wilson, H. F.; Lu, D.; Gygi, F.; Galli, G. *Phys. Rev. B* **2009**, *79*, 245106.
(14) Lu, D.; Nguyen, H.-V.; Galli, G. *J. Chem. Phys.* **2010**, *133*, 154110.
(15) Pham, T. A.; Li, T.; Shankar, S.; Gygi, F.; Galli, G. *Appl. Phys. Lett.* **2010**, *96*, 062902.
(16) Rocca, D.; Lu, D.; Galli, G. *J. Chem. Phys.* **2010**, *133*, 164109.
(17) Pham, T. A.; Li, T.; Shankar, S.; Gygi, F.; Galli, G. *Phys. Rev. B* **2011**, *84*, 045308.
(18) Kang, W.; Hybertsen, M. S. *Phys. Rev. B* **2010**, *82*, 195108.
(19) Benoit, D.; Sebastiani, D.; Parrinello, M. *Phys. Rev. Lett.* **2001**, *87*, 226401.
(20) Filippone, F.; Parrinello, M. *Chem. Phys. Lett.* **2001**, *345*, 179–182.
(21) Lanczos, C. *J. Res. Natl. Bur. Stand.* **1951**, *45*, 255–282.
(22) Saad, Y. *Numerical Methods for Large Nonsymmetric Eigenvalue Problems*, 1st ed.; Manchester University Press: Manchester, UK, 1992; pp 42−142.
(23) Hutter, J.; et al. *Computer code CPMD, version 3.12.0*; Copyright IBM Corp. and MPI-FKF Stuttgart, 1990−2007; http://www.cpmd.org, accessed 4/1/2011.
(24) Goedecker, S.; Teter, M.; Hutter, J. *Phys. Rev. B* **1996**, *54*, 1703–1710.
(25) Porezag, D.; Pederson, M. R. *Phys. Rev. B* **1996**, *54*, 7830–7836.